

# On Position and Attitude Estimation for Remote Sensing with Bistatic SAR

Stefan Knedlik, Junchuan Zhou and Otmar Loffeld  
Center for Sensorsystems (ZESS), University of Siegen  
Germany

## 1. Introduction

In recent years, there has been an increasing interest in remote sensing with bistatic SAR. Among the advantages bistatic SAR imaging offers in comparison to monostatic SAR imaging are that additional information can be exploited (specific bistatic angles can be chosen, and additional information is obtained from the bistatic reflectivity of targets and because of a reduction of di- and polyhedral effects), that SAR imaging along along-track direction will be feasible, that a cost reduction, as well as reduced size, weight, energy consumption can be achieved for passive receive-only systems, and that passive systems have a reduced vulnerability.

Several experiments have been carried out to prove the feasibility of remote sensing with bistatic SAR. While in the first experiments a stationary receiver or transmitter was involved or two airplanes (with almost parallel flight trajectories) have been used, so called hybrid experiments with Germany's national remote sensing satellite TerraSAR-X as illuminator and with an airborne SAR receiver system have been performed recently, and first processing results have been presented (cf. (Rodriguez-Cassola et al. 2008) or (Ender et al. 2006; Walterscheid et al. 2009) (where a larger bandwidth and a double sliding spotlight mode have been used)).

Among the research challenges in remote sensing with bistatic SAR are the derivation of proper processing algorithms (that yield focused images even in the most general case of arbitrary flight trajectories) and the *position and attitude determination of the SAR antennas* (with the accuracy and real-time ability required, and at relatively low cost).

Accurate position and attitude knowledge of the involved SAR antennas is required at several steps: It is an important issue in *footprint chasing*, that is, to obtain overlapped transmitter and receiver antenna footprints (by appropriate antenna steering) during the mission. In the hybrid experiments, the magnitude of the satellite velocity is about 76 times higher than that of the airplane. The overlap of the antenna footprints will be a few seconds in maximum (the operation in a double sliding spotlight mode is recommended). The aircraft has to fly over the target scene in time. Antenna steering can be used to compensate for smaller errors. The aircraft's trajectory and the attitude of its SAR antenna have to be known in real-time and typically absolute information is required (independent from the satellite (because the related information is not completely available from the satellite)). For

footprint chasing in such hybrid bistatic SAR experiments an antenna pointing error of about  $0.5^\circ$  in all the three angles is acceptable. The positioning requirements are even less strict.

Furthermore, accurate absolute position and attitude information is required for *motion compensation* and for *parameter estimation* (with respect to  $a_0$  = time difference parameter, and  $a_2$  = slant range ratio parameter (required during raw data processing)). Recently, in (Wang et al. 2009), the effect of uncompensated errors on the bistatic point target reference spectrum has been analyzed for the airborne/airborne case.

Absolute position and attitude information with highest accuracy is (in several applications) required for *geo-referencing*.

Moreover, in SAR interferometry the *baseline* (the vector between the antenna phase centers) has to be known. Depending on the parameters (e.g., wavelength, orbit) of illuminator and receiver, the baseline has to be estimated very accurately (e.g., with mm/cm (length) and arcsec (angle) accuracy, respectively) to obtain height errors smaller than 1 m. Here it is relative position and attitude information that is required (relative with respect to the carrier platforms), and here it is often not required in real-time.

The aforementioned position and attitude information can be obtained using inertial navigation or global navigation satellite systems (GNSS). In the following section, some fundamentals regarding these kinds of navigation are introduced, and the data fusion of corresponding measurements is considered. Example data fusion approaches for low cost position and attitude determination are given and analyzed in Section 3.

## 2. Introduction to GNSS/INS integration

### 2.1 Inertial navigation, satellite navigation, and its complementary characteristics

In inertial navigation, usually, *gyroscopes* and *accelerometers* are used, and they are mounted in triads so that the sensitive axes of the sensors are mutually orthogonal, setting up a Cartesian reference frame. In an *inertial measurement unit* (IMU), which contains the inertial sensor assembly, the raw data provided by the inertial sensors is converted to angular rates (from gyroscopes) and specific forces (from accelerometers), and typically an integration of the raw data over a certain time and also a calibration is performed. The output of an IMU are angular rates  $\omega_{ib}^b$  of the body-fixed frame (*b*-frame) with respect to the inertial frame (*i*-frame) (see subscript) given in the *b*-frame (superscript) and specific forces  $\mathbf{a}_{ib}^b$  (or, because of the integration, also delta-theta's and delta-V's, respectively). See Figure 1. These data can be processed yielding position, velocity, and attitude, which, in case of systems where the inertial sensor assembly is strapped down to a body frame of the host platform, has been coined *strapdown processing*. That is, starting from a known initial position, velocity, and attitude, dead reckoning is performed using the measurements of the inertial sensors. A system that contains an IMU and an appropriate processing unit has been coined *inertial navigation system* (INS). Strapdown inertial navigation is in detail explained in the literature. With an INS autonomous navigation (almost independent of the environment) at a high data rate (e.g., 100 Hz) can be realized. The full attitude information is available. However, the system has to be initialized, and information about the local gravity is required. Furthermore, due to the dead reckoning principle the errors are growing unbounded with

time. That is, even if expensive systems (e.g., with a price tag of 50.000\$–100.000\$) are used, position errors of about 1 km/h result if no calibration and external aiding is applied.

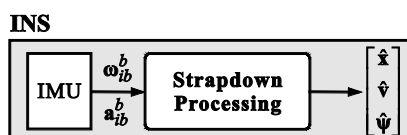


Fig. 1. Simplified block diagram of an inertial navigation system

Global navigation satellite systems (GNSS) such as the Global Positioning System (GPS) can be used to determine position, velocity, and time of a point on a platform. By measuring the time of arrival (TOA) and by using the transmission time, which can be extracted from the received signal, the propagation time and finally the range, the receiver-satellite distance, can be derived. By trilateration the receiver position can be determined. Typically, four or more simultaneous measurements are required to solve for the 3D receiver position and clock bias. The carrier phase/frequency and the code phase of the received signals are tracked by appropriate phase/frequency and delay lock loops. There is a correlation of the inphase (I) and quadrature phase (Q) components with replica signal quadrature components, and the I,Q samples are integrated and dumped. Phase/frequency of the replica carrier and phase of the replica code are the raw measurements of a GNSS receiver; and from these raw measurements pseudorange, delta range (or Doppler, carrier phase) and accumulated delta range (integrated Doppler) observations can be derived, and finally in a navigation processor (typically a Kalman filter) position, velocity, and time can be estimated based on the observations and a model of the dynamics (cf. Figure 2). More information about the systems, the signals, the error sources, the positioning methods (e.g., differential GNSS), and augmentation systems and services can be found in the literature.

GNSS based navigation is non-autonomous. Usually, at least 4 GNSS satellites have to be continuously in view. It is depending on the environment and there is a high vulnerability. On the other hand, one obtains absolute position, velocity and time information which is long-term stable. The output rate is relatively low (e.g., 1 Hz), and regarding the carrier phase measurements, the ambiguity resolution and the cycle slip detection and repair is challenging.

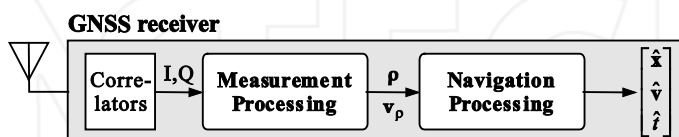


Fig. 2. Simplified block diagram of a GNSS receiver

As indicated above, GNSS based navigation and inertial navigation and the corresponding navigation solutions have *complementary characteristics*. Hence, GNSS/INS integration (in the sense of data fusion) is useful to obtain a complete and continuous navigation solution with high accuracy and high bandwidth at relatively low cost.

## 2.2 GNSS/INS integration approaches

Raw measurements and derived observations available from inertial navigation and GNSS based navigation, respectively, have been briefly mentioned in the preceding section.

From an information-theoretical point of view, it would be optimal if the raw measurements would be processed in a single centralized filter using, for example, a total state space model for the state space modelling. Especially if the  $I, Q$  components at the output of the correlators in the tracking loops are utilized, and if there is a feedback of the estimated Doppler from the fusion filter to the numerically-controlled oscillator (NCO) – which has been coined INS aiding GNSS – it is known as *deeply coupled* (or ultra-tightly coupled) GNSS/INS integration. (However, there is no commonly agreed definition of it). In that case, because of the INS aiding GNSS, only the residuals of the receiver dynamics have to be tracked in the tracking loops. The bandwidth is reduced, accuracy, and robustness can be improved, and the tracking can be faster. In practice, deeply coupled GNSS/INS integration is usually not applied. Access to the tracking loops of the GNSS receiver is usually not given. Moreover, there is a relatively high computational burden (e.g., from theory, a total state space model has to operate at a relatively high data rate) and relatively poor fault-tolerance. However, depending on the application (and specific requirements) it could outperform other approaches. In (Wagner and Wieneke 2003), the incorporation of the strapdown processing into the fusion filter and the use of a total state space filter have been proposed.

On the other hand, a decentralized, a distributed, estimation architecture can be considered which exploits the outputs of a GNSS receiver and of an INS. It is called a *loosely coupled* GNSS/INS integration architecture. Systems off-the-shelf can be used, and with the GNSS receiver and the INS independent and redundant navigation solutions are available. Drawbacks of a loosely coupled GNSS/INS integration are that typically four satellites have to be in view to obtain information from the GNSS receiver and that in case of a Kalman filter in the GNSS receiver (denoted by navigation processor in Figure 2) time correlated estimates of position and velocity are the input for the fusion filter (there are cascaded filters) which has to be accounted for (e.g., by considering this information only every  $>10$  s or by using a federated filter with high computational load). Moreover, cross correlations between position and velocity estimates exist, which can in practice often not be considered – because the belonging measurement noise covariance matrices are often not or not completely provided by the GNSS receiver – yielding a decreased performance.

Finally, one can distinguish a *tightly coupled* integration from the aforementioned approaches where pseudoranges and delta ranges or carrier phases (which are outputted by many GNSS receivers) are exploited. Different definitions of a tightly coupled GNSS/INS integration (e.g., with or without feedback to the GNSS receiver) can be found in the literature. In general, a tightly coupled filter is more complex (the fusion filter) than the loosely coupled filter but the estimation is more robust, and it is especially when signals from less than four satellites can be received superior.

Regarding the state space modelling, an *error state space model* is usually applied, which is also known as *indirect filtering*, cf. (Maybeck 1982). The strapdown processing based on the measurements of the inertial sensors is done separately at a high rate. It provides a reference trajectory. Measurements for the fusion filter are differences between GNSS receiver measurements and predicted measurements based on the INS output. The fusion filter operates at a relatively low rate at which GNSS based measurements are available. The

dynamics are given by the inertial error differential equations which can be well modelled as being linear.

The estimated errors are usually fed back to correct the IMU measurements yielding errors at the output of the INS which do not grow unbounded with time but remain small so that the assumption of a linear system model remains reasonable.

An exemplary GNSS/INS indirect feedback tightly coupled integration architecture is shown in Figure 3.

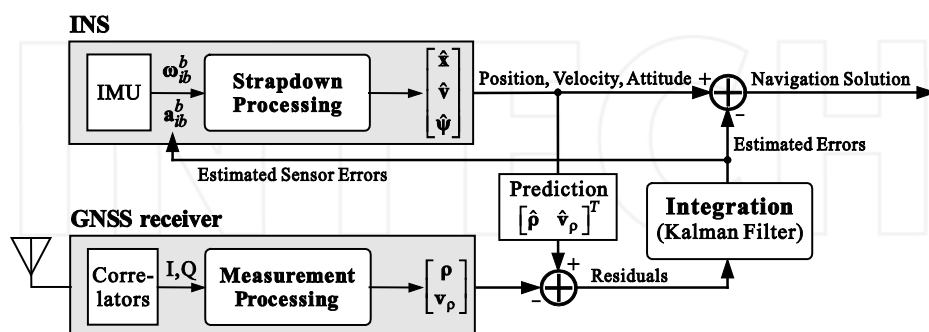


Fig. 3. GNSS/INS tightly coupled indirect feedback integration principle (example)

In general, the development of a proper GNSS/INS integration approach depends on the application. For example, the dynamics of the platform have to be taken into consideration (e.g., orbiting satellite versus unmanned aerial vehicle (UAV)) – not only for a possible modelling of the dynamics but also for a proper derivation and consideration of expected errors (e.g., with respect to multipath), required bandwidth and update rates, possible positioning or initialization methods, etc. Furthermore, among others, the structure of the platform has to be considered, the environment has to be considered, constraints can be derived and incorporated, and the grade of the inertial sensors and the GNSS receivers available has to be taken into consideration.

More details regarding GNSS/INS integration are given in the literature (e.g., (Farrell and Barth 1999)).

### 3. Low-cost GPS/INS integration with multiple GPS antennas

In this section, an example for GNSS/INS integration is given. GNSS/INS integration for position, velocity, and attitude estimation of an antenna mounted on an aircraft will be considered. The focus is on low cost. That is, a low-cost microelectromechanical system (MEMS) based IMU and L1 GPS receivers (that can output pseudorange, delta range, and carrier phase measurements) are supposed to be available.

*Tightly coupled GPS/INS indirect feedback* sensor data fusion approaches will be considered. Different proposals to integrate additional, redundant attitude information are compared.

#### 3.1 Preliminary considerations

The data fusion approaches are formulated with respect to the  $n$ -frame (with axes pointing locally north, east, down, respectively).

The error is defined as usual, that is, as observed or estimated value – true value.

The state vector for the tightly coupled integration is chosen to be

$$\Delta \mathbf{x}_c = \begin{bmatrix} [\Delta x_n^n & \Delta x_e^n & \Delta x_d^n]^T \\ [\Delta v_{eb,n}^n & \Delta v_{eb,e}^n & \Delta v_{eb,d}^n]^T \\ [\Delta \alpha & \Delta \beta & \Delta \gamma]^T \\ [\Delta b_{a,x} & \Delta b_{a,y} & \Delta b_{a,z}]^T \\ [\Delta b_{\omega,x} & \Delta b_{\omega,y} & \Delta b_{\omega,z}]^T \\ [c\Delta t_{rb} & c\Delta t_{rd}]^T \end{bmatrix} = \begin{bmatrix} \Delta \mathbf{x} \\ \Delta \mathbf{v} \\ \Delta \boldsymbol{\psi} \\ \Delta \mathbf{b}_a \\ \Delta \mathbf{b}_\omega \\ c\Delta t_r \end{bmatrix} \left\{ \begin{array}{l} \text{position error} \\ \text{velocity error} \\ \text{error in misalignment} \\ \text{accelerometer bias error} \\ \text{gyroscope bias error} \\ \text{receiver clock error} \end{array} \right. \quad (1)$$

That is, the state vector comprises 17 states.

Accelerometer levelling can be used to determine the initial bank angle (roll) and elevation angle (pitch) of the platform from the accelerometer measurements as follows

$$\theta = \arctan \left( -a_{ib,x}^b / \sqrt{(a_{ib,y}^b)^2 + (a_{ib,z}^b)^2} \right) \quad (2)$$

$$\varphi = \arctan_2 \left( a_{ib,y}^b / a_{ib,z}^b \right) \quad (3)$$

The MEMS-based IMU with a typical bias instability between several 100°/h and several 10000°/h can not sense Earth's rotation. Hence, gyro-compassing for alignment in azimuth can not be performed. Other sensors, such as a magnetometer, can be used to derive heading. Heading information can, for example, also be derived from GPS velocity measurements according to

$$\psi = \arctan_2(v_E / v_N) \quad (4)$$

or from *a priori* knowledge.

It can be shown by an observability analysis that only with additional redundant attitude information the states are completely observable (independent of the manoeuvre of the platform, dependent on the number of satellites in view).

This redundant attitude information can be provided by a multi-antenna GNSS receiver system. Here we use a non-dedicated system consisting of the master GPS receiver (including antenna) and two more (independent) GPS receivers (with antennas).

Because of an approximately straight and level flight, that can be assumed for a remote sensing experiment, the size effect related to the accelerometer triad can be neglected. Moreover, because of the low-cost IMU, in addition to other approximations (e.g., no Euler acceleration, that is, Earth's rotation rate assumed to be constant), the transport rate and Coriolis terms can be neglected in the strapdown processing and in the system model.

In subsequent sections, continuous-time models are provided. The appropriate discrete-time models can be derived as shown in the literature, e.g., in case of a time-variant system the state transition is described as

$$\begin{aligned}
 A(k) &= \phi((k+1)T, kT) = \phi(T) = e^{F((k+1)T - kT)} = e^{(F)T} \\
 &= \mathcal{L}^{-1} \left\{ [sI - F]^{-1} \right\} \Big|_{t=T} = I + F \cdot T + \frac{(F \cdot T)^2}{2} + \text{h.o.t.}
 \end{aligned} \quad (5)$$

where  $T$  is the sampling period. That is, if the continuous-time state transition matrix  $F(t)$  is time-invariant or only slightly varying with time, one can approximate

$$A(k) \approx I + F \cdot T \quad (6)$$

### 3.2 Strapdown mechanization

With aforementioned simplifications due to the characteristic of a low-cost IMU, the mechanization can be expressed as

$$\dot{\mathbf{x}}^n = \mathbf{v}^n \quad (7)$$

$$\dot{\mathbf{v}}^n = R_b^n \mathbf{a}_{ib}^b + \mathbf{g}_l^n \quad (8)$$

$$\dot{q}_b^n = \frac{1}{2} q_b^n \begin{bmatrix} 0 \\ \boldsymbol{\omega}_{nb}^b \end{bmatrix} = \frac{1}{2} q_b^n \begin{bmatrix} 0 \\ \boldsymbol{\omega}_{ib}^b \end{bmatrix} - \frac{1}{2} \begin{bmatrix} 0 \\ \boldsymbol{\omega}_{in}^n \end{bmatrix} q_b^n \approx \frac{1}{2} q_b^n \begin{bmatrix} 0 \\ \boldsymbol{\omega}_{ib}^b \end{bmatrix} \quad (9)$$

It is performed with the specific force vector  $\tilde{\mathbf{a}}_{ib}^b$ , related to the measurement of the accelerometer triad, with the angular rate vector  $\tilde{\boldsymbol{\omega}}_{ib}^b$ , related to the measurement of the gyroscopes, with the local gravity vector resolved in the  $n$ -frame  $\hat{\mathbf{g}}_l^n$ , and where  $\mathbf{x}$  (or  $\hat{\mathbf{x}}$ ) is (computed) position,  $\mathbf{v}$  (or  $\hat{\mathbf{v}}$ ) is (computed) velocity, and where the frame rotation from  $b$ -frame to  $n$ -frame is described by the computed direction cosine matrix  $\hat{R}_b^n$ . The computed platform rotation rate with respect to the inertial frame,  $\hat{\boldsymbol{\omega}}_{in}^n$ , is the sum of Earth's rotation rate (depending on latitude) and the transport rate (depending on the speed of the platform). Both contributions can be easily computed. Moreover, in some cases, depending on the application (gyroscope bias instability, velocity of the platform), these terms can be neglected. Note that the products in Eq. (9) are quaternion products as defined by Hamilton.

### 3.3 Error state system model

Because of the low-cost IMU, the uncompensated systematic error  $\Delta \mathbf{b}_a$  and  $\Delta \mathbf{b}_\omega$  in the measurements of the inertial sensors are considered as states, and they are modelled as random walk processes. The receiver clock drift (related to the frequency error) is modelled as constant plus a random walk process, and the clock bias  $c\Delta t_r$  (related to the phase error) is the integral of it.

With the aforementioned constraints and simplifications, the  $n$ -frame error state system model for the tightly coupled integration is set up as



$$\underbrace{\begin{bmatrix} \Delta \dot{\mathbf{x}} \\ \Delta \dot{\mathbf{v}} \\ \Delta \dot{\Psi} \\ \Delta \dot{\mathbf{b}}_a \\ \Delta \dot{\mathbf{b}}_\omega \\ c\Delta \dot{t}_r \\ c\Delta \dot{t}_r \end{bmatrix}}_{\Delta \mathbf{x}_c} = \underbrace{\begin{bmatrix} O & I & O & O & O & 0 & 0 \\ O & O & F_{23} & -\hat{R}_b^n & O & 0 & 0 \\ O & O & O & O & -\hat{R}_b^n & 0 & 0 \\ O & O & O & O & O & 0 & 0 \\ O & O & O & O & O & 0 & 0 \\ \mathbf{0}^T & \mathbf{0}^T & \mathbf{0}^T & \mathbf{0}^T & \mathbf{0}^T & 0 & 1 \\ \mathbf{0}^T & \mathbf{0}^T & \mathbf{0}^T & \mathbf{0}^T & \mathbf{0}^T & 0 & 0 \end{bmatrix}}_F \cdot \begin{bmatrix} \Delta \mathbf{x} \\ \Delta \mathbf{v} \\ \Delta \Psi \\ \Delta \mathbf{b}_a \\ \Delta \mathbf{b}_\omega \\ c\Delta t_r \\ c\Delta \dot{t}_r \end{bmatrix} + \mathbf{w} \quad (10)$$

where  $O$  and  $I$  denote a  $3 \times 3$  identity and  $3 \times 3$  zero matrix, respectively, and the sub-matrix  $F_{23}$  is a skew-symmetric matrix that contains the specific force components transformed to the  $n$ -frame

$$F_{23} = F_{a \times \psi} = [\hat{\mathbf{a}}_{ib}^n \times] = \begin{bmatrix} 0 & \hat{a}_{ib,d}^n & -\hat{a}_{ib,e}^n \\ -\hat{a}_{ib,d}^n & 0 & \hat{a}_{ib,n}^n \\ \hat{a}_{ib,e}^n & -\hat{a}_{ib,n}^n & 0 \end{bmatrix} \quad (11)$$

### 3.4 Observation models

In the tightly coupled integration the measurement vector contains the differences in predicted (based on strapdown solution for position and velocity) and measured pseudorange  $\rho$  and delta range  $v_\rho$ , respectively. Moreover, if redundant attitude information is available, e.g., derived from an independent GPS multiple-antenna system, the difference between predicted (from INS) and true attitude measurement can be included in the measurement vector. With respect to satellite number  $m$ , we have (in the  $n$ -frame)

$$\mathbf{y}_{t_1}^{(m)} = \begin{bmatrix} \hat{\rho}^{(m)} - \tilde{\rho}^{(m)} \\ \hat{v}_\rho^{(m)} - \tilde{v}_\rho^{(m)} \\ \hat{\Psi} - \tilde{\Psi} \end{bmatrix} \quad (12)$$

In the tightly coupled integration, the states are *nonlinearly* mapped into the observation space. Hence, an extended Kalman filter can be used for the estimation of the states. The Jacobian has to be computed. The resulting observation matrix, that maps the 17 state vector components (Eq. (1)) into observation space, is

$$H_{t_1}^{(m)} = \begin{bmatrix} -(\mathbf{1}_t^{(m),n})^T & \mathbf{0}^T & \mathbf{0}^T & \mathbf{0}^T & \mathbf{0}^T & 1 & 0 \\ \mathbf{0}^T & -(\mathbf{1}_t^{(m),n})^T & \mathbf{0}^T & \mathbf{0}^T & \mathbf{0}^T & 0 & 1 \\ O & O & R & O & O & 0 & 0 \end{bmatrix} \quad (13)$$



where  $\mathbf{1}_t^{(m),n}$  is the unit vector in the line of sight from receiver (master GPS antenna A0) to satellite number  $m$ , resolved in the  $n$ -frame, and where  $R$  is a frame rotation matrix for the transformation from body-axes angular rates to the Euler angle angular rates.

The matrix has the dimension  $(3 + \nu \cdot 2) \times 17$ , where  $\nu$  is the number of satellites in view.

Sequential processing has to be performed to avoid inversion of a huge matrix.

If the redundant attitude information is obtained from a multi-antenna GPS receiver system we can, instead of first computing the attitude, directly exploit the double-difference carrier phase measurements of the system. This kind of integration of the attitude information from a GPS multiple-antenna system has been proposed in (Hirokawa and Ebinuma 2009). In the measurement vector we have then rather differences of predicted and present double-difference carrier phase measurements (related to antennas A0, A1, and A2) than the difference in attitude. In case of two satellites,  $m$  and  $n$ , the measurement vector is given as

$$\mathbf{y}_{t_2}^{(m,n)} = \begin{bmatrix} \hat{\rho}^{(m)} - \tilde{\rho}^{(m)} \\ \hat{\varphi}_{\rho}^{(m)} - \tilde{\varphi}_{\rho}^{(m)} \\ \hat{\rho}^{(n)} - \tilde{\rho}^{(n)} \\ \hat{\varphi}_{\rho}^{(n)} - \tilde{\varphi}_{\rho}^{(n)} \\ \nabla \Delta \hat{\phi}_{A0,A1}^{(n,m)} - \nabla \Delta \tilde{\phi}_{A0,A1}^{(n,m)} \\ \nabla \Delta \hat{\phi}_{A0,A2}^{(n,m)} - \nabla \Delta \tilde{\phi}_{A0,A2}^{(n,m)} \end{bmatrix} \quad (14)$$

where the symbols in parentheses represent satellites (and where the time index has again been neglected for convenience). The true double-difference carrier phase observation can be expressed as shown by the following example:

$$\begin{aligned} \nabla \Delta \phi_{A0,A1}^{(n,m)} &= \frac{2\pi}{\lambda} \left[ \left( \rho_{A1}^{(n)} - \rho_{A1}^{(m)} \right) - \left( \rho_{A0}^{(n)} - \rho_{A0}^{(m)} \right) \right] \\ &= \frac{2\pi}{\lambda} \left[ \left( \rho_{A1}^{(n)} - \rho_{A0}^{(n)} \right) - \left( \rho_{A1}^{(m)} - \rho_{A0}^{(m)} \right) \right] \end{aligned} \quad (15)$$

and the measured double-difference carrier phase can be modelled as

$$\nabla \Delta \tilde{\phi}_{A0,A1}^{(n,m)} = \frac{2\pi}{\lambda} \cdot \nabla \Delta \rho_{A0,A1}^{(n,m)} + \frac{2\pi}{\lambda} \cdot c \cdot \nabla \Delta \text{MP}_{\phi,A0,A1}^{(n,m)} + e_{\phi \nabla \Delta} - 2\pi \cdot \nabla \Delta N_{A0,A1}^{(n,m)} \quad (16)$$

where besides the integer ambiguity  $\nabla \Delta N$ , only the non-common mode errors multipath  $\nabla \Delta \text{MP}$  and receiver noise  $e_{\phi \nabla \Delta}$  have to be considered.

As soon as there is another satellite in view, the measurement vector is augmented by four more rows (pseudorange and delta range differences to the new satellite, respectively, and new double-difference carrier phase measurements related to the master satellite  $m$ ).

In case of  $\nu > 1$  satellites in view, we obtain obviously a  $(2 + (\nu - 1) \cdot 4) \times 17$  matrix that relates the 17 state vector components to the observations. The Jacobian, the observation matrix, corresponding to Eq. (14) (2 satellites in view) is

$$H_{t_2}^{(m,n)} = \begin{bmatrix} -(\mathbf{1}_t^{(m,n)})^T & \mathbf{0}^T & \mathbf{0}^T & \mathbf{0}^T & \mathbf{0}^T & 1 & 0 \\ \mathbf{0}^T & -(\mathbf{1}_t^{(m,n)})^T & \mathbf{0}^T & \mathbf{0}^T & \mathbf{0}^T & 0 & 1 \\ -(\mathbf{1}_t^{(n,n)})^T & \mathbf{0}^T & \mathbf{0}^T & \mathbf{0}^T & \mathbf{0}^T & 1 & 0 \\ \mathbf{0}^T & -(\mathbf{1}_t^{(n,n)})^T & \mathbf{0}^T & \mathbf{0}^T & \mathbf{0}^T & 0 & 1 \\ \mathbf{0}^T & \mathbf{0}^T & \frac{2\pi}{\lambda} (\mathbf{1}_t^{(m,n)} - \mathbf{1}_t^{(n,n)})^T [\hat{R}_b^n \mathbf{1}_{01}^b \times] & \mathbf{0}^T & \mathbf{0}^T & 0 & 0 \\ \mathbf{0}^T & \mathbf{0}^T & \frac{2\pi}{\lambda} (\mathbf{1}_t^{(m,n)} - \mathbf{1}_t^{(n,n)})^T [\hat{R}_b^n \mathbf{1}_{02}^b \times] & \mathbf{0}^T & \mathbf{0}^T & 0 & 0 \end{bmatrix} \quad (17)$$

where  $\mathbf{1}_t^{(m,n)}$  is the unit vector in the line of sight from master antenna (A0) to satellite  $m$ , resolved in the  $n$ -frame, and  $\mathbf{1}_{0i}^b$  is the lever arm (baseline) between the phase centers of master antenna (A0) and antenna number  $i$ , known in the  $b$ -frame.

### 3.5 Further remarks to the integration approach

Derivations of the Kalman filter and its augmentations for nonlinear models as well as the resulting algorithms are not repeated here. The reader is for example referred to (Maybeck 1982), (Simon 2006).

The measurements from the IMU or from the inertial navigation system can be expected with a high data rate (e.g., 100 Hz), which is much higher than the data rate of the measurements derived from GPS. Hence, to reduce the computational burden, to obtain a filter that operates at a relatively low rate, the measurements from the inertial sensors are not incorporated as measurements (cf. Section 3.4). Instead, they are directly used in the strapdown processing to predict position, velocity, and attitude. In addition, only the *a priori* error covariance matrix  $P^-(k)$  has to be predicted as usual (in the *prediction* step, and not necessarily at the high data rate).

As soon as a new measurement vector can be computed, that is, as soon as information from GPS is available, the error state is estimated, and the state vector is *corrected*. In case of small rotations there is approximately no difference between the components of the rotation vector and the Euler angles. That is, the estimated attitude error can be interpreted as rotation vector, and the correction of the *a priori* attitude quaternion is done by computing the quaternion product  $\hat{q}_{b,k}^{n,+} = \hat{q}_{b,k}^{n,-} q_k^n$ , where the  $n$ -frame rotation quaternion is computed with  $\boldsymbol{\phi} = -\Delta\hat{\boldsymbol{\psi}}$ ,  $\phi = \sqrt{\boldsymbol{\phi}^T \boldsymbol{\phi}}$  and with  $q^n = [\cos(\phi/2) \quad \sin(\phi/2)\boldsymbol{\phi}/\phi]^T$  (using a Taylor series approximation). The correction of the other states is straightforward (subtraction of the appropriate estimated error state). After the correction, the errors state is zeroed.

### 3.6 Simulation setup and results

For the following experiments a *hardware-in-the-loop* system has been used for the GPS part. It consists of the RF GPS signal simulator system NavX-NCS from Ifen GmbH and Novatel DL-4 plus GPS receivers. Synthetic inertial measurements (as obtained from a low-cost IMU)

have been generated using the parameters of a typical consumer grade IMU (cf. Table 1). A straight and level flight with a nominally constant velocity of 110 m/s in east has been modelled. The parameters describing the experiment are given in Table 1.

Trajectory		
Velocity (ENU) [m/s]	$\mathbf{v}^E = [110 \quad 0 \quad 0]^T$	
Initial Position ( $\varphi, \lambda, h$ )	$\mathbf{x}^e = [51^\circ\text{N} \quad 8^\circ\text{E} \quad 3 \text{ km}]^T$	
Angles ( $\varphi, \theta, \psi$ ) [ $^\circ$ ]	$\boldsymbol{\psi} = [0 \quad 0 \quad 90]^T$	
Start Time (UTC)	October 29, 2006, 00:11:27	
Duration	180 s	
GPS measurements		
Update rate	1 Hz	
Measurements	Depending on integration approach: code pseudo-range, delta range, (double-differenced carrier phase)	
Method	Point positioning, and attitude determination from a non-dedicated multiple antenna system (3 antenna-receiver pairs with baselines of 2 m each)	
Error modelling	Tropospheric delay is estimated and corrected for; The small ionospheric delay is estimated and corrected for; No multipath (calibrated out); Ambiguities resolved and cycle slips repaired (assumed)	
Satellites in view	2–8 (as depicted in Figs. 4–5)	
Elevation angle	$\geq 5^\circ$	
IMU measurements		
Update rate	100 Hz	
Error modelling	<i>Gyroscope (Angular rates)</i>	
	Bias stability [ $^\circ/\text{h}$ ]	360
	Scale factor [ppm]	10000
	Noise (ARW) [ $^\circ/\text{h}/\sqrt{\text{Hz}}$ ]	180
	<i>Accelerometer</i>	
	Bias stability [ $\mu\text{g}$ ]	2400
	Scale factor [ppm]	10000
	Noise (VRW) [ $\mu\text{g}/\sqrt{\text{Hz}}$ ]	1000

Table 1. Nominal parameters describing the setup

An extended Kalman filter has been used for the GPS/INS integration which is based on the state space modelling provided in Sections 3.1–3.5. An ideal time-synchronization has been assumed, time-delayed measurements have not been taken into consideration. An initialization has been performed as described in Section 3.1. The attitude estimation results are depicted in Figure 4.

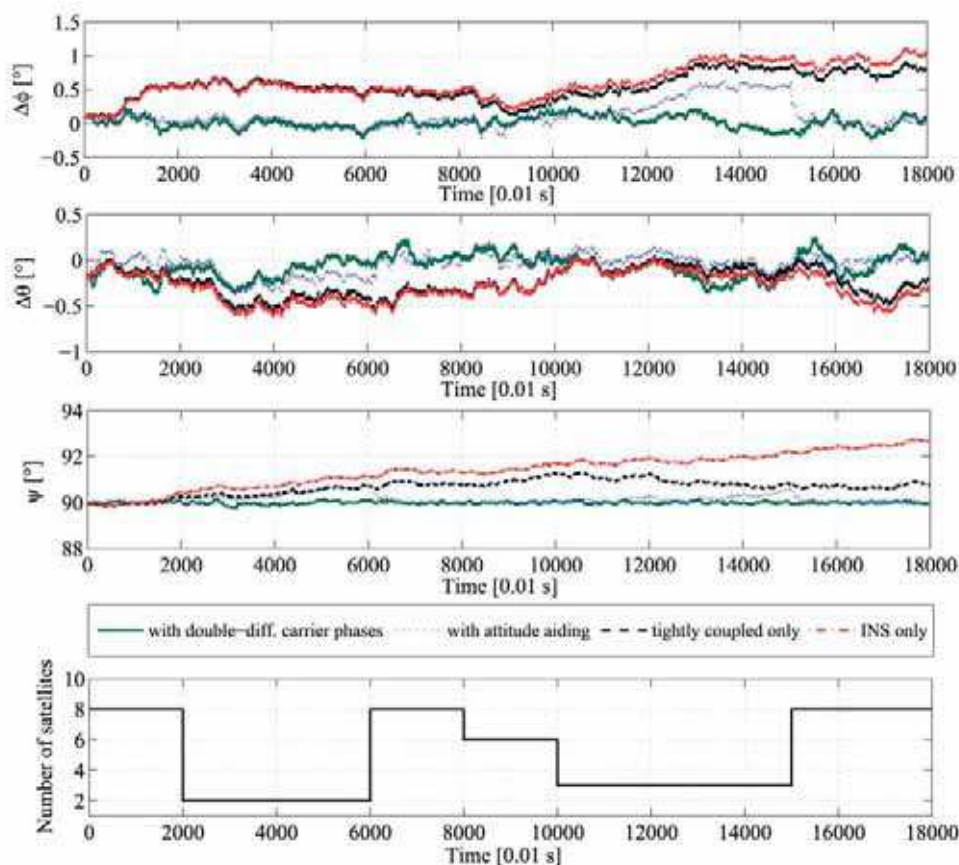


Fig. 4. Attitude estimation result using tightly coupled GPS/INS integration approaches

Because of the proper initialization (including an estimation of the gyroscope bias instability and an appropriate correction) of the IMU, the errors are relatively small, that is, after 3 minutes (180 s) the heading error is in case of the stand-alone IMU still smaller than  $3^\circ$ . Without initialization and calibration the error would be larger than  $20^\circ$ . As expected, in case of the stand-alone IMU, the largest error can be observed in heading.

In the tightly coupled GPS/INS integration without redundant attitude information the attitude errors (and sensor biases) are not directly mapped into observation space. However, these error states will also be updated with every new position and velocity measurement. These quantities are related to each other as shown by the system model, and this is reflected in the predicted error covariance matrix (used for computing the Kalman gain). It is therefore no surprise that the attitude estimation results using a tightly coupled GPS/INS integration (represented by the black, dashed curves in Figure 4) are better than using a similar INS alone.

A much more accurate attitude estimation result is obtained using additional redundant attitude information (shown by blue dotted lines in Figure 4). The measurement vector is

then given by Eq. (12). The redundant attitude information is here obtained from a multiple antenna GPS receiver system. In case of less than 4 satellites in view, the system can not provide attitude information. Hence, the errors become much larger during such periods. Finally, if the double-difference carrier phase measurements from the non-dedicated multi-antenna system are used (with the observation matrix given by Eqs. (17) (for the case of two satellites)) the results are comparable in case of four or more satellites in view, but if only two or three satellites are in view still a robust and accurate attitude information is obtained. In Figure 5, the obtained position, velocity, and attitude errors are shown.

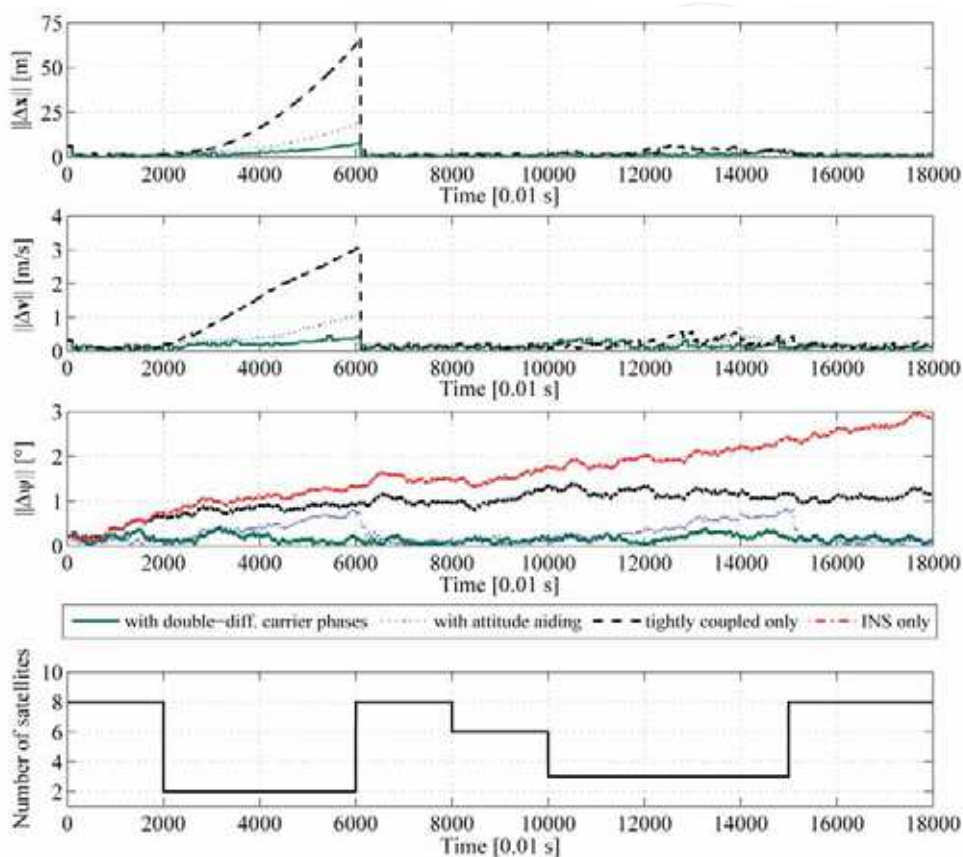


Fig. 5. Navigation solution using tightly coupled GPS/INS integration approaches

The large stand-alone IMU related position and velocity errors (about 1 km and 15 m/s after 3 minutes, respectively) are not included in the figure. In general, if only two satellites are in view, the position and velocity errors grow remarkably. During the period where only three satellites are in view, the position and velocity errors are bounded (which is not the case in a loosely coupled GPS/INS integration). Again, the incorporation of the double-difference carrier phase measurements into the integration approach yields the best results.

### 3.7 Conclusions

Tightly coupled indirect feedback GNSS/INS integration approaches have been compared in Section 3. Required additional redundant attitude information can be derived from GNSS using three antenna-receiver pairs. In that case, the double-difference carrier phase measurements should be directly incorporated into the integration approach, as has been shown by looking at approaches for low-cost GPS/INS integration and appropriate simulation results. Such approaches and low-cost sensors can for example be used for footprint chasing in bistatic SAR.

Carrier phase measurements have to be exploited to achieve the required attitude estimation accuracy. The detection and repair of cycle slips and the rapid integer ambiguity resolution are challenging. It is easier if shorter baselines are used (because of a reduced search space), however, the longer the baselines the better the expected attitude accuracy.

The lever arm between specific force origin of the IMU and phase center of the main GNSS antenna can be easily incorporated.

Depending on the application, the assumptions have to be proven. For example, delayed measurements have to be considered, and depending on the platform (e.g., UAV) multipath errors that can not be calibrated are an issue, and unconsidered flexure and vibrations can remarkably decrease the accuracy.

Constraints, such as that an airplane is in straight and level flight during a remote sensing experiment, can be easily incorporated into the estimation approach.

A novel GNSS/INS direct integration approach that exploits direction cosine matrix orthogonality constraints and that incorporates a model of the dynamics has been proposed recently (Edwan et al. 2009).

The redundant attitude information required can possibly also be derived from a comparison of a quick-look SAR image with an existing digital map.

To obtain more accurate position and attitude estimates, an IMU of a higher grade and precise point positioning can be exploited.

## 4. Summary

The importance of accurate and reliable attitude and position information for remote sensing with bistatic SAR has been pointed out in the introduction. In the following section, inertial navigation and navigation based on global navigation satellite systems have been mentioned. Reasons for GNSS/INS integration have been provided, and appropriate data fusion architectures have been briefly introduced and discussed. In the main section, low-cost tightly coupled GPS/INS integration approaches with and without additional redundant attitude information have been presented, and simulation results have been discussed.

## 5. Acknowledgements

Part of the work reported herein has been funded by the German Research Foundation (DFG), grant number KN 876/1-2, which is gratefully acknowledged.

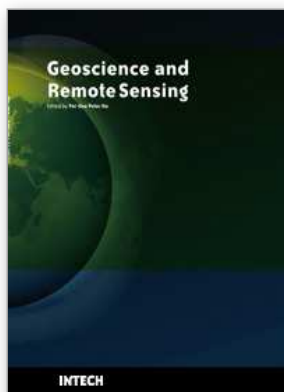
## 6. References

- Edwan, E., Knedlik, S., Zhou, J., and Loffeld, O. (2009). "Constrained GPS/INS integration based on rotation angle for attitude update and dynamic models for position update." *ION ITM 2009 (The Institute of Navigation International Technical Meeting)*, Anaheim, CA, USA.
- Ender, J. H. G., Loffeld, O., Brenner, A. R., Wiechert, W., Klare, J., Gebhardt, U., Walterscheid, I., Knedlik, S., Weiss, M., Nies, H., Kirchner, C., Kalkuhl, M., Wilden, H., Natroshvili, K., Medrano-Ortiz, A., Amankwah, A., Kolb, A., and Ige, S. (2006). "Bistatic exploration using spaceborne and airborne SAR sensors - A close collaboration between FGAN, ZESS and FOMAAS." *IGARSS 2006 (IEEE International Geoscience and Remote Sensing Symposium)*, Denver, Colorado, USA.
- Farrell, J. A., and Barth, M. (1999). *The global positioning system and inertial navigation*, McGraw-Hill, New York.
- Hirokawa, R., and Ebinuma, T. (2009). "A low-cost tightly coupled GPS/INS for small UAVs augmented with multiple GPS antennas." *Navigation: Journal of The Institute of Navigation*, 56(1), 35-44.
- Maybeck, P. S. (1982). *Stochastic models, estimation, and control (Vol. I, II)*, Academic Press, New York.
- Rodriguez-Cassola, M., Baumgartner, S. V., Krieger, G., Nottensteiner, A., Horn, R., Steinbrecher, U., Metzger, R., Limbach, M., Prats, P., Fischer, J., Schwerdt, M., and Moreira, A. (2008). "Bistatic spaceborne-airborne experiment TerraSAR-X/F-SAR: data processing and results." *IGARSS 2008 (IEEE International Geoscience and Remote Sensing Symposium)*, III - 451-III - 454.
- Simon, D. (2006). *Optimal state estimation: Kalman, H infinity, and nonlinear approaches*, Wiley-Interscience, Hoboken, N.J.
- Wagner, J. F., and Wieneke, T. (2003). "Integrating satellite and inertial navigation - conventional and new fusion approaches." *Control Engineering Practice*, 11, 543-550.
- Walterscheid, I., Espeter, T., Brenner, A. R., Klare, J., Ender, J. H. G., Nies, H., Wang, R., and Loffeld, O. (2009). "Bistatic SAR experiment with PAMIR and TerraSAR-X - setup, processing, and image results." *IEEE Transactions on Geoscience and Remote Sensing*, under review.
- Wang, R., Loffeld, O., Nies, H., Medrano Ortiz, A., and Knedlik, S. (2009). "Bistatic point target reference spectrum in the presence of trajectories deviations." *IET Radar, Sonar & Navigation*, 3(2), 177-185.



INTECH

INTECH



## **Geoscience and Remote Sensing**

Edited by Pei-Gee Peter Ho

ISBN 978-953-307-003-2

Hard cover, 598 pages

**Publisher** InTech

**Published online** 01, October, 2009

**Published in print edition** October, 2009

Remote Sensing is collecting and interpreting information on targets without being in physical contact with the objects. Aircraft, satellites ...etc are the major platforms for remote sensing observations. Unlike electrical, magnetic and gravity surveys that measure force fields, remote sensing technology is commonly referred to methods that employ electromagnetic energy as radio waves, light and heat as the means of detecting and measuring target characteristics. Geoscience is a study of nature world from the core of the earth, to the depths of oceans and to the outer space. This branch of study can help mitigate volcanic eruptions, floods, landslides ... etc terrible human life disaster and help develop ground water, mineral ores, fossil fuels and construction materials. Also, it studies physical, chemical reactions to understand the distribution of the nature resources. Therefore, the geoscience encompass earth, atmospheric, oceanography, pedology, petrology, mineralogy, hydrology and geology. This book covers latest and futuristic developments in remote sensing novel theory and applications by numerous scholars, researchers and experts. It is organized into 26 excellent chapters which include optical and infrared modeling, microwave scattering propagation, forests and vegetation, soils, ocean temperature, geographic information , object classification, data mining, image processing, passive optical sensor, multispectral and hyperspectral sensing, lidar, radiometer instruments, calibration, active microwave and SAR processing. Last but not the least, this book presented chapters that highlight frontier works in remote sensing information processing. I am very pleased to have leaders in the field to prepare and contribute their most current research and development work. Although no attempt is made to cover every topic in remote sensing and geoscience, these entire 26 remote sensing technology chapters shall give readers a good insight. All topics listed are equal important and significant.

### **How to reference**

In order to correctly reference this scholarly work, feel free to copy and paste the following:

Stefan Knedlik, Junchuan Zhou and Otmar Loffeld (2009). On Position and Attitude Estimation for Remote Sensing with Bistatic SAR, *Geoscience and Remote Sensing*, Pei-Gee Peter Ho (Ed.), ISBN: 978-953-307-003-2, InTech, Available from: <http://www.intechopen.com/books/geoscience-and-remote-sensing/on-position-and-attitude-estimation-for-remote-sensing-with-bistatic-sar>

**INTECH**  
open science | open minds

### **InTech Europe**

University Campus STeP Ri  
Slavka Krautzeka 83/A

### **InTech China**

Unit 405, Office Block, Hotel Equatorial Shanghai  
No.65, Yan An Road (West), Shanghai, 200040, China

51000 Rijeka, Croatia  
Phone: +385 (51) 770 447  
Fax: +385 (51) 686 166  
[www.intechopen.com](http://www.intechopen.com)

中国上海市延安西路65号上海国际贵都大饭店办公楼405单元  
Phone: +86-21-62489820  
Fax: +86-21-62489821

INTECH

INTECH